Diffusion of Probe Molecule in Small Liquid *n*-Alkanes:
A Molecular Dynamics Simulation Study

Choong-Do Yoo, Soon-Chul Kim,[†] and Song Hi Lee[*]

Department of Chemistry, Kyungsung University, Busan 608-736, Korea. [*]E-mail: shlee@ks.ac.kr
[†]Department of Physics, Andong National University, Andong 760-749, Korea

The probe diffusion and friction constants of methyl yellow (MY) in liquid *n*-alkanes of increasing chain length were calculated by equilibrium molecular dynamics (MD) simulations at temperatures of 318, 418, 518 and 618 K. Lennard-Jones particles with masses of 225 and 114 g/mol are modeled for MY. We observed that the diffusion constant of the probe molecule follows a power law dependence on the molecular weight of *n*-alkanes, $D_{MY} \sim M^{-\gamma}$ well. As the molecular weight of *n*-alkanes increases, the exponent γ shows sharp transitions near *n*-dotriacontane (C_{32}) for the large probe molecule (MY2) at low temperatures of 318 and 418 K. For the small probe molecule (MY1) D_{MY1} in C_{12} to C_{80} at all the temperatures are always larger than D_{self} of *n*-alkanes and longer chain *n*-alkanes offer a reduced friction relative to the shorter chain *n*-alkanes, but this reduction in the microscopic friction for MY1 is not large enough to cause a transition in the power law exponent in the log-log plot of D_{MY1} *vs* M of *n*-alkane. For the large probe molecule (MY2) at high temperatures, the situation is very similar to that for MY1. At low temperatures and at low molecular weights of *n*-alkanes, D_{MY2} are smaller than D_{self} of *n*-alkanes due to the relatively large molecular size of MY2, and MY2 experiences the full shear viscosity of the medium. As the molecular weight of *n*-alkane increases, D_{self} of *n*-alkanes decreases much faster than D_{MY2} and at the higher molecular weights of *n*-alkane, MY2 diffuses faster than the solvent fluctuations. Therefore there is a large reduction of friction in longer chains compared to the shorter chains, which enhances the diffusion of MY2. The calculated friction constants of MY1 and MY2 in liquid *n*-alkanes supported these observations. We deem that this is the origin of the so-called "solvent-oligomer" transition.

Key Words : Molecular dynamics simulation, Probe molecule, *n*-Alkanes, Diffusion, Friction

Introduction

Fundamental understanding of diffusion of small probe molecules in polymer films and bulk polymers are of great importance because of the information they provide on local segmental motions of polymer molecules at high polymer concentrations or in undiluted state.[1,2] In the past two decades, molecular dynamics (MD) simulation methods have been a common tool to study structural and dynamical properties of macromolecules[3] and to study the behavior of small probe molecules in polymers.[4] Due to the connectivity of N monomeric units, characteristic relaxation times τ of polymers are very large and scale as $\tau \sim N^2$ for short chains, and as $\tau \sim N^{3.4}$ for entangled chains. As a consequence, polymer melts have difficult configurational spaces which severely complicate the study of the ensemble properties of such systems.

In a recent paper,[5] diffusion of methyl yellow (MY) in the oligomeric host of *n*-alkanes and *n*-alcohols was studied by forced Rayleigh scattering as a function of the molecular weight and the viscosity of the medium. It was observed that the diffusion constant of the probe molecule follows a power law dependence on the molecular weight of the oligomers, $D_{MY} \sim M^{-\gamma}$ well. As the molecular weight of the oligomers increases, the exponent γ shows a sharp transition from 1.88 to 0.91 near docosane (C_{22}) in *n*-alkanes and from 1.31 to

0.60 near 1-hexadecanol ($C_{16}OH$) in *n*-alcohols at 45 °C. A similar transition is also found in the molecular dynamics simulation for the diffusion of a Lennard-Jones particle of a size similar to MY in *n*-alkanes. This transition deems to reflect a change of the dynamics of oligomeric chain molecules that the motion of the segments, not the entire molecules, becomes responsible for the transport of the probe molecule as the molecular weight of the oligomer increases.

In the present paper, we report new results of equilibrium molecular dynamics (MD) simulations for probe molecules in small liquid *n*-alkanes at several temperatures of 318, 418, 518, and 618 K. We have chosen 9 liquid *n*-alkanes of various chain lengths, $12 \leq N \leq 80$. The primary study goal is to analyze the diffusion and friction dynamics of probe molecules in *n*-alkanes at different temperatures. In general, the smaller the probe molecules is, the smaller the exponent, γ, is. For example, carbon dioxide shows an exponent of 0.44 in various organic solvents.[6] We try to investigate the exponent dependence on the molecular size of the probe relative to the molecular size of the diffusing media. In the primary MD simulation for diffusion of a probe molecule,[5] the system considered was at the temperature of 318 K only. We also try to investigate the exponent dependence of the probe diffusion in liquid *n*-alkanes on the temperature.

Since the diffusion of the probe molecule reflects the local friction of the diffusing medium, one of the experimental

methods to obtain the monomeric friction constant ζ_o is to measure the friction constant of probe molecules in polymeric media.[2,7-9] It is also well established experimentally that the diffusion constant of a probe molecule in polymer solutions is independent of the matrix polymer molecular weight at the Rouse regime.[7-9] In this study, we calculate the friction constant of the probe molecule and investigate the friction effect of liquid *n*-alkanes on the probe diffusion.

Molecular Models and Molecular Dynamics Simulation

To calculate the diffusion constant of methyl yellow (MY) with molecular weight of 225 g/mol in *n*-alkane matrices, we carried out MD simulations for the systems which consist of a Lennard-Jones (LJ) particle and N = 100 of *n*-alkane molecules with different carbon numbers. The LJ particle modeled for the probe interacts with all the interaction sites of *n*-alkanes with LJ potential parameters of $\sigma = 6.0$ Å and $\varepsilon = 0.6$ kJ/mol (labeled as MY2). In order to study the size effect of the probe particle, we further carried out MD simulations for a smaller size of LJ particle of LJ potential parameters of $\sigma = 4.0$ Å and $\varepsilon = 0.4$ kJ/mol with molecular weight of 114 g/mol (labeled as MY1).

For liquid *n*-alkanes, we have chosen 9 systems - *n*-dodecane ($C_{12}H_{26}$), *n*-hexadecane ($C_{16}H_{34}$), *n*-eicosane ($C_{20}H_{42}$), *n*-tetracosane ($C_{24}H_{50}$), *n*-octacosane ($C_{28}H_{58}$), *n*-dotriacontane ($C_{32}H_{66}$), *n*-hexatriacontane ($C_{36}H_{74}$), *n*-tetratetracontane ($C_{44}H_{90}$), and *n*-tetratetracontane ($C_{80}H_{162}$). Each simulation was carried out in the NpT ensemble with the probe molecule at the center of the simulation box to determine the volume of each system at given temperatures, and after the equilibrium density and hence the length of cubic simulation box were obtained, new NVT MD simulation was performed for each system to store the configurations of the probe molecule and *n*-alkanes for later analyses. The usual periodic boundary condition in the x-, y-, and z-directions and the minimum image convention for pair potential were applied. Gaussian isokinetics was used to keep the temperature of the system constant.[10,11]

We used a united atom (UA) model for *n*-alkanes, that is, methyl and methylene groups are considered as spherical interaction sites centered at each carbon atom. This model was used in the previous simulation studies.[12-16] Here we briefly describe the salient features of the model. The interaction between the sites on different *n*-alkane molecules and between the sites separated by more than three bonds in the same *n*-alkane molecule was described by a Lennard-Jones (LJ) potential. All the sites in a chain have the same LJ size parameter $\sigma_i \equiv \sigma_{ii} = 3.93$ Å, and the well depth parameters were $\varepsilon_i \equiv \varepsilon_{ii} = 0.94784$ kJ/mol for interactions between the end sites and $\varepsilon_i = 0.39078$ kJ/mol for interactions between the internal sites. The Lorentz-Berthelot combining rules [$\varepsilon_{ij} \equiv (\varepsilon_i\varepsilon_j)^{1/2}$, $\sigma_{ij}(\sigma_i + \sigma_j)/2$] were used for interactions between an end site and an internal site, and between the probe LJ particle and all the sites of *n*-alkanes. A cut-off distance of $2.5\sigma_i$ was used for all the LJ interactions.

Initially the bond-stretching was described by a harmonic

potential, with an equilibrium bond distance of 1.54 Å and a force constant of 1882.8 kJ/mol·Å^2. The bond bending interaction was also described by a harmonic potential with an equilibrium angle of 114° and a force constant of 0.079187 kJ/mol·degree.[2] The torsional interaction was described by the potential developed by Jorgensen *et al.*:[17]

$$U_{torsion}(\phi) = a_0 + a_1 \cos\phi + a_2 \cos^2\phi + a_3 \cos^3\phi. \qquad (1)$$

where ϕ is the dihedral angle, and $a_0 = 8.3973$ kJ/mol, $a_1 = 16.7862$ kJ/mol, $a_2 = 1.1339$ kJ/mol, and $a_3 = -26.3174$ kJ/mol. For the time integration of the equations of motion, we adopted Gear's fifth-order predictor-corrector algorithm[18] with a time step of 0.5 femto-second for all the systems. Later the bond-stretching was switched to a constraint force which keeps intramolecular nearest neighbors at a fixed distance. The advantage for this change is to increase the time step as 5 femto-seconds with the use of RATTLE algorithm.[19] After a total of 1,000,000 time steps (5 nanoseconds) for equilibration, the equilibrium properties were then averaged over 5 blocks of 200,000 time steps (1 nanosecond). The configurations of all the molecules for further analyses were stored every 10 time steps (0.05 pico second) which is small enough for the tick of any time auto-correlation functions.

Self-diffusion constant (D_{self}) of liquid *n*-alkane and diffusion constant (D_{MY}) of the probe LJ particle can be obtained through the Green-Kubo formula from velocity auto-correlation function (VAC):

$$D = \frac{1}{3}\int_0^\infty dt \langle \mathbf{v}_i(0) \cdot \mathbf{v}_i(t) \rangle. \qquad (2)$$

Shear viscosity (η) of liquid *n*-alkane is also calculated through the Green-Kubo formula from stress auto-correlation function (SAC):

$$\eta = \frac{V}{kT}\int_0^\infty dt \langle P_{\alpha\beta}(0) \cdot P_{\alpha\beta}(t) \rangle, \qquad (3)$$

where $P_{\alpha\beta}$ is the $\alpha\beta$ component of the molecular stress tensor, **P**:

$$P_{\alpha\beta}(t) = \frac{1}{V}\sum_i \left[mv_{i\alpha}(t)v_{i\beta}(t) + \sum_{j \neq i} r_{ij\alpha}(t)f_{ij\beta}(t) \right], \qquad (4)$$

where $\alpha\beta = $ xy, xz, yx, yz, zx, or zy.

A microscopic expression for the friction constant has been obtained through a Green-Kubo formula by Kirkwood[20] from the time integral of the force auto-correlation (FAC) function[21,22] in the form:

$$\zeta = \frac{1}{\tau_r} = \frac{1}{3kT}\int_0^\tau dt \langle \mathbf{f}_i(0) \cdot \mathbf{f}_i(t) \rangle, \qquad (5)$$

where $\mathbf{f}_i(t) = \mathbf{F}_i(t) - \langle \mathbf{F}_i(t) \rangle$, $\mathbf{F}_i(t)$ is the total force exerted on molecule *i* and τ_r is the macroscopic relaxation time of the FAC.[22]

Results and Discussion

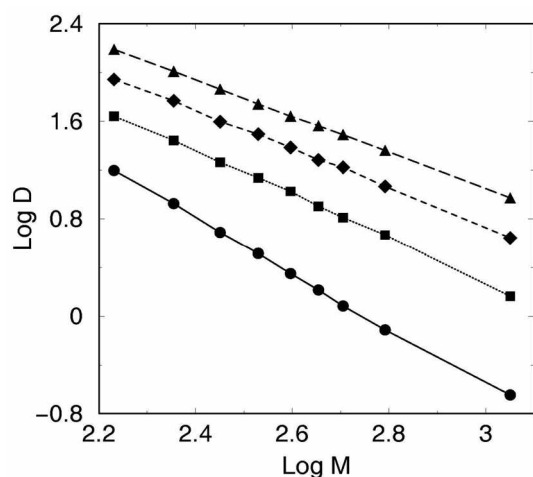Self-diffusion constants of liquid *n*-alkanes are obtained

Figure 1. A log-log plot of $D_{self}(10^{-5} cm^2/s)$ *vs* M (g/mol). From top, T = 618 (▲), 518 (◆), 418 (■), and 318 K (●), respectively.

from velocity auto-correlation (VAC) function through the Green-Kubo formula. Eq. (2), at four different temperatures and the log-log plot of self-diffusion constant (D_{self}) versus the molecular weight (M) is shown in Figure 1. The slopes are almost linear at given temperatures and this indicates that the behavior of D_{self} *vs* M is well described by $D_{self} \sim M^{-\alpha}$. The obtained exponents are 2.28 (318 K), 1.80 (418 K), 1.59 (518 K), and 1.48 (618 K). At the molecular weight below the Rouse regime. D_{self} of *n*-alkanes also show power law behaviors. For example, D_{self} of *n*-alkanes for *n*-octane to polyethylene of the molecular weight of several thousands was reported that the exponents α is in the range of 2.72-1.75 depending on temperature.[23-25] Our previous MD simulation study[26] for *n*-$C_{12} \sim C_{44}$ at T = 273-473 K is another examples and the obtained exponents were between 2.43 (273 K) and 1.58 (473 K). Apparently the exponent in liquid *n*-alkanes decreases with increasing temperature. Independence of self-diffusion constant of liquid *n*-alkane on the molecular weight is expected at very high temperatures.
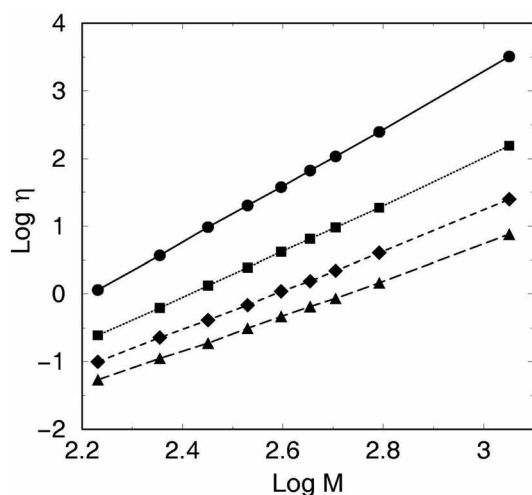
Viscosities of liquid *n*-alkanes are obtained from stress auto-correlation (SAC) function through the Green-Kubo formula, Eq. (3), at four different temperatures and Figure 2 shows the log-log plot of viscosity (η) versus the molecular weight (M). The slopes are also almost linear at given temperatures and this indicates that the behavior of η *vs* M is well described by $\eta \sim M^\beta$. The obtained exponents are 4.20 (318 K), 3.41 (418 K), 2.92 (518 K), and 2.61 (618 K). The experimental results for *n*-alkanes and linear polyethylene[24] show that η is also well described by the power law: $\eta \sim M^{1.8}$ at low molecular weight (M < 5 kg/mol) and $\eta \sim M^{3.6}$ at high molecular weight (M > 5 kg/mol) at 448 K. Our previous MD simulation study[26] for *n*-$C_{12} \sim C_{44}$ at T = 273-473 K gives the exponents between 3.70 (273 K) and 1.97 (473 K). The exponent in the log-log plot of η *vs* M decreases with increasing temperature as well as that in the log-log plot of D_{self} *vs* M, but the exponents. $-\alpha$ and β, have opposite signs.

The temperature dependence of the calculated self-diffusion constants of liquid *n*-alkanes on the whole temperatures considered is suitably described by an Arrhenius plot. $D_{self} = D_0 \exp(-E_{D,self}/RT)$. as shown in Figure 3. where D_0 is the pre-exponential factor, RT has the usual meaning. and $E_{D,self}$ is the activation energy of *n*-alkane self-diffusion. The value of the activation energy is a direct measure of how fast the self-diffusion changes with temperature. The activation energies obtained from the slope of the least square fit are between 2.95 (C_{12}) and 4.85 kcal/mol (C_{80}). Our previous MD simulation study[26] for liquid *n*-$C_{12} \sim C_{44}$ at T = 273-473 K gives the activation energies of 2.83, 3.52, 3.91, and 4.06 kcal/mol for C_{12}, C_{20}, C_{32}, and C_{44}. respectively. $E_{D,self}$ is small for small *n*-alkanes. The values of $E_{D,self}$ are plotted in Figure 4 as function of chain length, N. As chain length N increases the increment of $E_{D,self}$ decreases. and it is expected to approach an asymptotic value as N increases further. It was reported that $E_{D,self}$ increases linearly with log M from 2.32 kcal/mol for *n*-heptane to 5.81 kcal/mol for *n*-hexacontane (C_{60}).[25,27] Fleischer[23] also determined $E_{D,self}$ to be about 4.8 kcal/mol for several polyethylene independent of
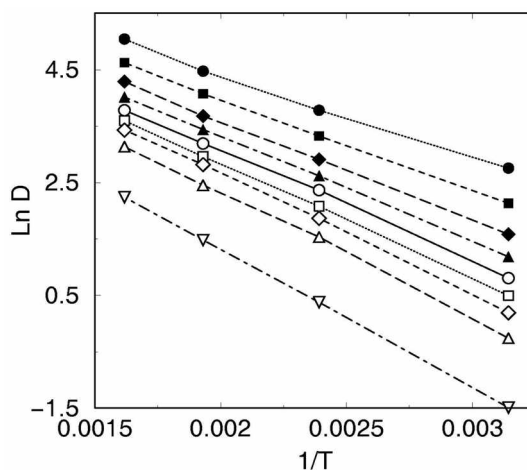

Figure 2. A log-log plot of η(cp) *vs* M (g/mol). From top, T = 318 (●), 418 (■), 518 (◆), and 618 K (▲), respectively.

Figure 3. Arrhenius plot of D_{self} ($10^{-5} cm^2/s$) *vs* 1/T. From top, $C_{12} \sim C_{80}$.
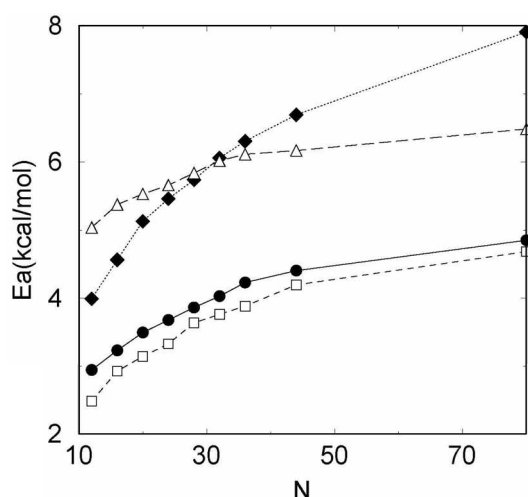
Figure 4. Activation energies (kcal/mol) of D_{self} for liquid *n*-alkanes (●), D_{MY1} (□), D_{MY2} (△), and of η for liquid *n*-alkanes (◆) *vs* carbon number N.

molecular weight from 9 to 52.7 kg/mol, from which we can deduce that $E_{D,self}$ of *n*-alkane reaches an asymptotic limit over C_{60}.

We also show the temperature dependence of the calculated viscosities of liquid *n*-alkanes on the temperatures which is also suitably described by an Arrhenius plot. $\eta = \eta_0 \exp(E_\eta/RT)$, as shown in Figure 5: where η_0 is the pre-exponential factor and E_η is the activation energy of *n*-alkane viscosity. The activation energies obtained from the slope of the least square fit are between 3.99 (C_{12}) and 7.91 kcal/mol (C_{80}) as shown in Figure 4. Our previous MD simulation study[26] for liquid *n*-$C_{12} \sim C_{44}$ at T = 273-473 K gives the activation energies of 2.33, 3.29, 4.63, and 5.46 kcal/mol for C_{12}, C_{20}, C_{32}, and C_{44}, respectively. E_η is also small for small *n*-alkanes. In Figure 4 the E_η increases continuously with the chain length N. However, it is expected that E_η would eventually reach an asymptotic value as N increases further based on the following results in the literature, but the value will be much higher than that of D_{self}
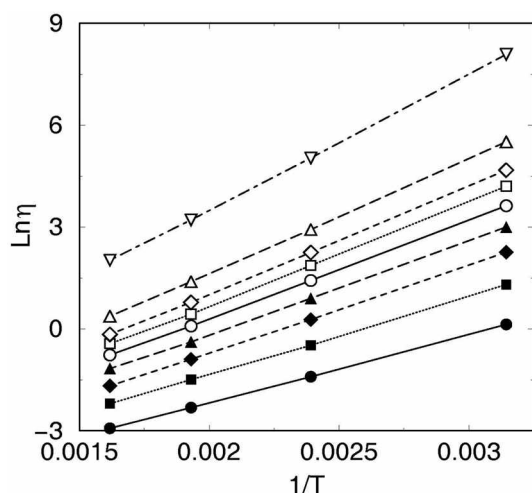

Figure 5. Arrhenius plot of η (cp) *vs* 1/T. From top, $C_{80} \sim C_{12}$.

as seen in Figure 4. It was experimentally reported for *n*-alkanes and linear polyethylene[24] that the activation energy increases with chain length and at the highest molecular weight tested (M ~ 4.4 kg/mol) the activation energy reaches 6.6 kcal/mol. which is similar to the average value found for NBS 1482-4 (6.7 kcal/mol) and the values reported by others[28,29] for high molecular weight linear polyethylene (6.1-6.9 kcal/mol).

Figures 6 and 7 show the dependence of D_{MY} on the molecular weight of liquid *n*-alkane at four different temperatures for the two probes. MY1 (the smaller probe) and MY2 (the larger probe), respectively. and the corresponding plots of D_{self} of *n*-alkane for comparison. Clearly D_{MY} for both probes decreases with the molecular weight of *n*-alkane according to the power law. $D_{MY} \sim M^{-\alpha}$. Such a power law dependence has been observed earlier for the probe diffusion in small molecular liquids. For example, diffusion constants of Me_4Sn (molecular weight of 178.7 g/mol) show the exponent of 1.9 in n-alkanes (from *n*-hexane to *n*-hexadecane) at 298 K.[30,31] This value is in agreement with the exponent found with MY1 (molecular weight of 114 g/mol) in the $C_{12} \sim C_{80}$ *n*-alkanes. 1.2 at 318 K. The values of the other exponents obtained for MY1 are $\gamma = 0.80$ (418 K), 0.50 (518 K), and 0.27 (618 K), which are much smaller than those for D_{self} of the *n*-alkanes as compared in Figure 6.

Unlike the linear behavior in the log-log plot of D_{MY1} *vs* M of *n*-alkane in Figure 6, a transition in the power law exponent is observed in the same plot for MY2 at low temperatures in Figure 7. However, the transitions at high temperatures of 618 and 518 K are not clear. Since there is a single probe molecule in each simulation, the statistical treatment for D_{MY} is very poor. The transitions at the low temperatures of 418 and 318 K seem rather obvious and the transition points are near *n*-dotriacontane (C_{32}). The calculated exponents are 1.21 and 0.63 in the low- and high-molecular weight regions. respectively, at 418 K, and 1.59 and 0.70 at 318 K. Those were 1.58 and 0.52 with the
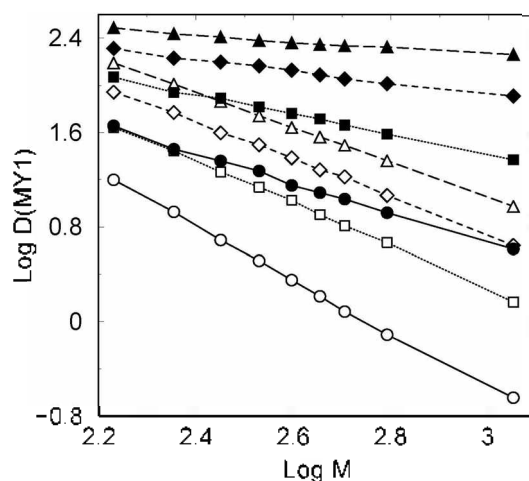

Figure 6. A log-log plot of D_{MY1} (10^{-6} cm²/s) *vs* M (g/mol) of *n*-alkane. From top, T = 618 (▲), 518 (◆), 418 (■), and 318 K (●), respectively (black symbols), and the corresponding plot of D_{self} *vs* M of *n*-alkane (white symbols).

Figure 7. A log-log plot of D_{MY2} (10^{-6} cm²/s) *vs* M (g/mol) of *n*-alkane. From top, T = 618 (▲), 518 (◆), 418 (■), and 318 K (●), respectively (black symbols), and the corresponding plot of D_{self} *vs* M of *n*-alkane (white symbols).
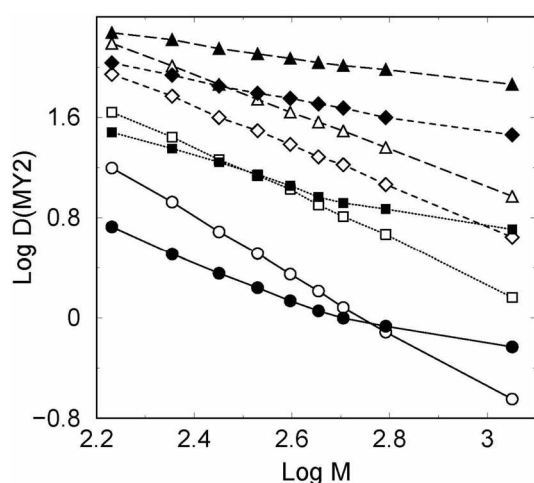
transition point at C_{24} in a previous MD simulation study of N = 27 *n*-alkane molecules[5] at 318 K, and the experimentally measured values are 1.88 and 0.91 with the transition point at C_{22} at 318 K.[5] Assuming the log-log plot of D_{MY2} *vs* M of *n*-alkane at 618 and 518 K in Figure 7 as straight lines, the corresponding exponents are 0.51 and 0.71, respectively, and comparing these values with those for MY1 at the same temperatures – 0.27 and 0.50, we found that the smaller the probe is the smaller the exponent is. This is in a good agreement with the existing experimental results for the probe diffusion in small molecular liquid.[6,30,31] For example, carbon dioxide shows an exponent of 0.44 in various organic solvents.[6]

It is interesting to compare D_{MY} for both probe molecules in *n*-alkanes with D_{self} of *n*-alkanes, denoted black and white symbols at each temperature in Figures 6 and 7. For MY1, D_{MY1} are always larger than D_{self} at all the temperatures due to the relatively small molecular size of MY1. As the molecular weight of *n*-alkane increases, D_{MY1} decreases much slower than D_{self} and two diffusion constants never cross each other. In the context of the Brownian motion that is behind any diffusion process, processes slower than or comparable to solvent fluctuations will be affected by the full spectrum of the solvent fluctuations and experience the full shear viscosity of the medium. On the other hand, processes much faster than the solvent fluctuations do not experience the Brownian fluctuating force and are not viscously damped. The case of MY1 belongs to the latter. Thus one expects a reduction in the microscopic friction for the probe molecules that diffuse at a rate faster than the solvent fluctuations.[32] Therefore, for small solute molecules which diffuse in a time scale shorter than the solvent fluctuations, longer chain *n*-alkanes offer a reduced friction relative to the shorter chain *n*-alkanes.

D_{MY2} are always larger than D_{self} at the high temperatures of 618 and 518 K, and D_{MY2} and D_{self} never cross each other as well as in D_{MY1} at all the temperatures. At low temper-

atures of 418 and 318 K, D_{MY2} and D_{self} cross each other. At 418 K, D_{MY2} in C_{12} to C_{20} is smaller than D_{self} of C_{12} to C_{20}, D_{MY2} in C_{24} is almost equal to D_{self} of C_{24}, and D_{MY2} in C_{28} to C_{80} are larger than D_{self} of C_{28} to C_{80}. The slope in the log-log plot of D_{self} *vs* M is −1.80 up to C_{80}, but the corresponding slope of D_{MY2} is −1.21 up to C_{32} and −0.63 from C_{32} to C_{80}. At 318 K, the same kind of transition is observed in which D_{MY2} is smaller than D_{self} except for C_{44} and C_{80}. The slope in the log-log plot of D_{self} *vs* M is −2.28 up to C_{80}, but the corresponding slope of D_{MY2} is −1.59 up to C_{32} and −0.70 from C_{32} to C_{80}. Clearly the transition is related to the size of probe molecule and temperature. As discussed above, one expects the reduced friction in longer chains compared to the shorter chains for small solute molecules which diffuse faster than the solvent fluctuations. On the other hand, solute molecules slower than or comparable to solvent fluctuations will be affected by the full spectrum of the solvent fluctuations and experience the full shear viscosity of the medium. One expects no such transition for a molecule large enough to experience the full friction of the medium in both short and long chains. We call the molecular weight regime of *n*-alkane at each side of the transition point as the "solvent" and "oligomer" regimes. As the molecular weight of liquid *n*-alkane is increased further, we can expect another transition from the oligomer to the "polymer" regime where the molecular weight dependence of the probe diffusion disappears. It was shown experimentally that the diffusion constant of small molecules in polymer solutions of sufficiently large molecular weight is nearly independent on the molecular weight or viscosity of the polymers.[7] MD simulations for much longer *n*-alkane chains like $C_{100} \sim C_{400}$ are presently under study.

We calculated the diffusional activation energies ($E_{D,MY}$) of both MY's in liquid *n*-alkanes. The temperature dependence of D_{self} and η of *n*-alkanes is well described by the Arrhenius equation as shown Figures 3 and 5, and that of D_{MY} in *n*-alkanes is also well described by the equation (not shown). Both $E_{D,MY}$ in liquid *n*-alkanes are acquired from the slope of the Arrhenius plot and Figure 4 shows the molecular weight dependence of $E_{D,MY}$ in *n*-alkanes. The values of $E_{D,MY1}$ in all the *n*-alkanes are always slightly less than $E_{D,self}$ of *n*-alkanes, and the behavior of $E_{D,MY1}$ is very similar to that of $E_{D,self}$ as function of the molecular weight of *n*-alkane. This indicates that MY1 diffuses more easily than *n*-alkane molecules at all the temperatures and D_{MY1} is always larger than D_{self} as seen in Figure 6, and processes faster than the solvent fluctuations do not experience the Brownian fluctuating force as discussed above.

On the contrary, the values of $E_{D,MY2}$ in all the *n*-alkanes are always larger than those of $E_{D,self}$. The E_{η} in of C_{12} is much smaller than $E_{D,MY2}$ in C_{12}. As the chain length of *n*-alkane increases, E_{η} of *n*-alkane increases faster than $E_{D,MY2}$ and E_{η} becomes slightly larger than $E_{D,MY2}$ at C_{32}, which is the solvent-oligomer transition point of D_{MY2} in *n*-alkane at the low temperatures. It is also expected that as the chain length of *n*-alkane increases, both $E_{D,MY}$ reach asymptotic values, which are approximately estimated as 5.0 and 6.5

kcal/mol, respectively.

Molecular friction constants of both *n*-alkanes and probe molecules are calculated from their force auto-correlation functions (FAC) obtained from our MD simulations using Eq. (5). The FAC function for center of mass of *n*-alkane shows a well-behaved smoothly decaying curve, while those for center and end monomers are oscillating ones probably due to the rapidly varying interaction of methyl (or methylene) groups and it is impossible to calculate the monomeric friction constants of center directly from the FAC of each monomer. The initial decay of the FAC for center of mass of *n*-alkane is very rapid to a deep negative well, occurring in a time ~0.2 ps, while a subsequent long tail decays only after several ps (not shown). The FAC of probe molecules are very similar to that of center of mass of *n*-alkane except much shallower negative wells (not shown).

As Kubo pointed out in his "fluctuation-dissipation theorem",[22] the correlation function of random force R will decay in a time interval of τ_c (microscopic time or collision duration time), whereas that of the total force F has two parts, the short time part or the fast similar to that of the random force and the slow part which should just cancel the fast part in the time integration.[33] This means that the time integral of Eq. (5) up to $\tau = \infty$ is equal to zero. The time integral in Eq. (5) attains a plateau value for τ satisfying $\tau_c \ll \tau \ll \tau_r$, if the upper limit of the time integral, Eq. (5), is chosen that $\tau_c \ll \tau \ll \tau_r$ because the slow tail of the correlation function is cut off. However, we were unable to get the plateau value in the running time integral of the force auto-correlation function. Kubo suggested that the friction constants should be obtained from the random FAC function not from the total FAC and that there exists a difficulty to separate the random force part from the total force. We could obtain the friction constants by the time integral of the total FAC choosing the upper limit of τ as the time which the FAC has the first negative value by assuming that the fast random force correlation ends at that time as proposed by Lagr'kov and Sergeev.[34]

The obtained friction constant (z) of center of mass of *n*-alkane is plotted as function of molecular weight of liquid *n*-alkane in the log-log plot as shown in Figure 8. The slopes are almost linear at given temperatures and this indicates that the behavior of ζ *vs* M is well described by $\zeta \sim M^\delta$. The obtained exponents are between 1.03 (318 K) and 1.09 (618 K) which indicates the independence of ζ on the temperature unlike D_{self}. The friction on the center of mass of *n*-alkane comes from the motion of the whole chain and it is expected that the friction constant increases linearly with the chain length of *n*-alkane. In Figure 9 the log-log plot of friction constant (ζ_{MY}) versus the molecular weight (M) of *n*-alkane is plotted to show how the friction of probe molecules changes as function of chain length of liquid *n*-alkane. For the smaller probe molecule, MY1, the obtained slope in the form of (log $\zeta_{MY1} \sim \delta$ log M) increases almost linearly up to C_{24} and the increment of the slope decreases from C_{28} to C_{80} at all the temperatures as the chain length of *n*-alkane increases. This is the manifestation of the reduced friction in
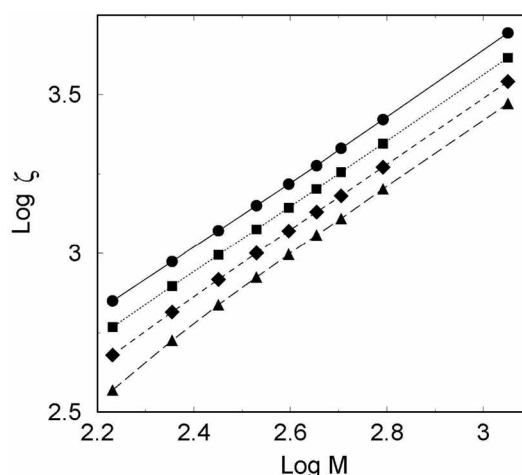

Figure 8. A log-log plot of ζ(g/ps·mol) of center of mass of *n*-alkane *vs* M (g/mol). From top, T = 318 K (●), 418 (■), 518 (◆), and 618 (▲), respectively.

longer chains compared to the shorter chains for small solute molecules which diffuse faster than the solvent fluctuations. However, the reduction in the microscopic friction for the probe molecules is not large enough to cause a transition in the power law exponent in the log-log plot of D_{MY1} *vs* M of *n*-alkane as shown in Figure 6.

For the larger probe molecule, MY2, the calculated friction constants are much larger than those of MY1 at all the temperatures. At high temperatures of 518 and 618 K, the behavior of the slope in the log-log plot of ζ_{MY2} *vs* M is very similar to that of MY1 except that the clear change of slope from the assumed linear dependence of the friction of MY2 on the chain length of *n*-alkane starts at C_{36} instead of C_{28} in the case of MY1 and that the initial slopes in the log-log plot of ζ_{MY2} *vs* M at high temperatures are larger than those in the log-log plot of ζ_{MY1} *vs* M at all the temperatures. We believe that this is due to the size of the probe molecule. We also believe that the friction of *n*-alkane solvent for MY diffusion
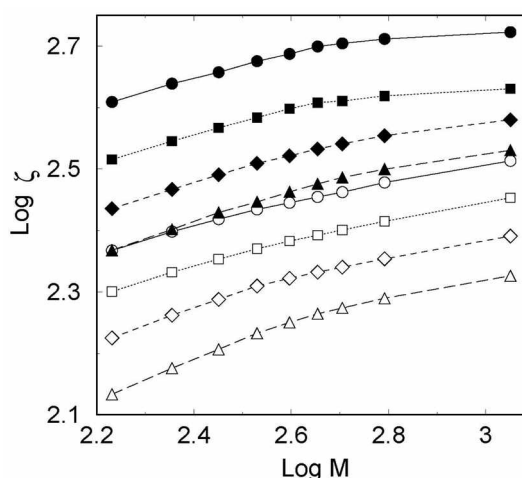

Figure 9. A log-log plot of ζ(g/ps·mol) of MY1 and MY2 *vs* M (g/mol). From top, T = 318 K (●), 418 (■), 518 (◆), and 618 (▲) for MY2, and T = 318 K (○), 418 (□), 518 ( ), and 618 (△) for MY1, respectively.

comes from the segmental motion of the chain, not from the motion of the whole chain.

For MY2 at low temperatures of 318 and 418 K, a large deviation of slope from the linear dependence of the friction of MY2 on the chain length of n-alkane starting at C_{36} is found, but the initial slopes in the log-log plot of ζ_{MY2} vs M are almost equal at all the temperatures. This is another manifestation that solute molecules slower than or comparable to solvent fluctuations will be affected by the full spectrum of the solvent fluctuations and experience the full shear viscosity of the medium. As the molecular weight of n-alkane increases, D_{self} of n-alkanes decreases much faster than D_{MY2} and at the higher molecular weights of n-alkane, MY2 diffuses faster than the solvent fluctuations. Therefore there is a large reduction of friction in longer chains compared to the shorter chains, which enhances the diffusion of the probe molecules, MY2. We believe that this is the origin of the "solvent-oligomer" transition as seen in Figure 7.

Conclusion

We have extended equilibrium molecular dynamics (MD) simulations for the probe diffusion and friction dynamics of Lennard-Jones (LJ) particles modeled for methyl yellow (MY) in liquid n-alkanes at temperatures of 318, 418, 518, and 618 K to investigate the size effect of probe molecule and the temperature effect. Two LJ particles are chosen: MY1 with mass of 114 g/mol and LJ parameters of $\sigma = 4.0$ Å and $\varepsilon = 0.4$ kJ/mol. and MY2 of 225 g/mol and $\sigma = 6.0$ Å and $\varepsilon = 0.6$ kJ/mol.

We observed that the diffusion constant of the probe molecule follows a power law dependence on the molecular weight of n-alkanes, $D_{MY} \sim M^{-\gamma}$ well. The exponent γ decreases as the temperature increases, and the smaller the probe is the smaller the exponent is. We also observed a clear transition in the power law dependence of MY2 diffusion on the molecular weight of n-alkanes at lower temperatures of 318 and 418 K. The sharp transitions occur near n-dotriacontane (C_{32}) at both temperatures. However, no such transition is found for MY1 at all the temperatures and for MY2 at higher temperatures of 518 and 618 K. Clearly the transition is related to the size of probe molecule and temperature.

We also calculated the friction constants of both MY probe molecules in liquid n-alkane. For the larger probe molecule, MY2, at low temperatures, a large deviation of slope from the linear dependence of the friction of MY2 on the chain length of n-alkane is found, which indicates a large reduction of friction in longer chains compared to the shorter chains, enhancing the diffusion of the probe molecules. MY2. However, for MY1 at all the temperatures and for MY2 at high temperatures, the reduction in the microscopic friction for the probe molecules is not large enough to cause a transition in the power law exponent in the log-log plot of D_{MY1} vs M of n-alkane.

References

1. Fujita, H. *Adv. Polym. Sci.* **1961.** *3*, 1.
2. Ferry, J. D. *Viscoelastic Properties of Polymers.* 3rd ed.; Wiley: New York, 1980.
3. Epameinondas, E.; Forrest, B. M.; Widmann, A. H.; Sulter, U. W. *J. Chem. Soc., Faraday Trans.* **1995.** *91*, 2355; Forrest, B. M.; Sulter, U. W. *J. Chem. Phys.* **1994.** *101*, 2616.
4. Gusev, A. A.; Müller-Plathe, F.; van Gunstern, W. F.; Sulter, U. W. *Adv. Polym. Sci.* **1994.** *116*, 207; Müller-Plathe, F. *Acta Polym.* **1994.** *45*, 259.
5. Park, H. S.; Chang, T.; Lee, S. H. *J. Chem. Phys.* **2000.** *113*, 5502.
6. Hayduck, W.; Cheng, S. C. *Chem. Eng. Sci.* **1971.** *26*, 635.
7. Gisser, D. J.; Johnson, B. S.; Ediger, M. D.; von Meerwall, E. D. *Macromolecules* **1993.** *26*, 512.
8. von Meerwall, E. D.; Amis, E. J.; Ferry, J. D. *Macromolecules* **1985.** *18*, 260.
9. Landry, M. R.; Gu, Q.; Yu, H. *Macromolecules* **1988.** *21*, 1158.
10. Evans, D. J.; Hoover, W. G.; Failor, B. H.; Moran, B.; Ladd, A. J. C. *Phys. Rev.* **1983.** *A28*, 1016.
11. Simmons, A. J. D.; Cummings, P. T. *Chem. Phys. Lett.* **1986.** *129*, 92.
12. Siepmann, J. I.; Karaborni, S.; Smit, B. *Nature* (London) **1993.** *365*, 330.
13. Smit, B.; Karaborni, S.; Siepmann, J. I. *J. Chem. Phys.* **1995.** *102*, 2126.
14. Mundy, C. J.; Siepmann, J. I.; Klein, M. L. *J. Chem. Phys.* **1995.** *102*, 3376.
15. Cui, S. T.; Cummings, P. T.; Cochran, H. D. *J. Chem. Phys.* **1996.** *104*, 255.
16. Cui, S. T.; Gupta, S. A.; Cummings, P. T.; Cochran, H. D. *J. Chem. Phys.* **1996.** *105*, 1214.
17. Jorgensen, W. L.; Madura, J. D.; Swenson, C. J. *J. Am. Chem. Soc.* **1984.** *106*, 6638.
18. Gear, C. W. *Numerical Initial Value Problems in Ordinary Differential Equation*, Prentice-Hall: Englewood Cliffs, 1971.
19. Andersen, H. *J. Comput. Phys.* **1984.** *52*, 24.
20. Kirkwood, J. *J. Chem. Phys.* **1946.** *14*, 180.
21. Ciccotti, G.; Ferrario, M.; Hynes, J. T.; Kapral, R. *J. Chem. Phys.* **1990.** *93*, 7137.
22. Kubo, R. *Rep. Prog. Phys.* **1966.** *29*, 255.
23. Fleisher, G. *Polymer Bulletin* (Berlin) **1983.** *9*, 152.
24. Pearson, D. S.; Ver Strate, G.; von Meerwall, E.; Schilling, F. C. *Macromolecules* **1987.** *20*, 1133.
25. Von Meerwall, E.; Beckman, S.; Jang, J.; Mattice, W. L. *J. Chem. Phys.* **1998.** *108*, 4299.
26. Lee, S. H.; Chang, T. *Bull. Korean Chem. Soc.* **2003.** *24*, 1590.
27. Ertl, H.; Dullien, F. A. L. *AIChE J.* **1973.** *19*, 1215.
28. Mendelson, R. A.; Bowles, W. A.; Finer, F. L. *J. Polym. Sci. Part A-2* **1970.** *8*, 105.
29. Raju, V. R.; Smith, G. G.; Marin, G.; Knox, J. R.; Graessley, W. W. *J. Polym. Sci., Polym. Phys. Ed.* **1979.** *17*, 1183.
30. Evans, D. F.; Tominaga, T.; Davis, H. T. *J. Chem. Phys.* **1981.** *74*, 1298.
31. Chen, S.-H.; Davis, H. T.; Evans, D. F. *J. Chem. Phys.* **1982.** *77*, 2540.
32. Ben-Amotz, D.; Scott, T. W. *J. Chem. Phys.* **1987.** *87*, 3739.
33. Kubo approximately described these two force auto-correlation functions in his original papers. see Fig. 2 in Ref. 22.
34. Lagar'kov, A. N.; Sergeev, V. H. *Usp. Fiz. Nauk.* **1978.** *125*, 409 [*Sov. Phys. Usp.* **1978.** *21*, 566].